

# Casein Micelles at Non-Ambient Pressure Studied by Neutron Scattering

R. H. Tromp · T. Huppertz · J. Kohlbrecher

Received: 9 April 2014 / Accepted: 21 July 2014 / Published online: 1 August 2014  
© Springer Science+Business Media New York 2014

**Abstract** The disruption of casein micelles, as found in cows' milk, was investigated at pressures up to 300 MPa with small angle neutron scattering (SANS). From the decrease of the overall level of scattering, the expected disruption of the micelles was concluded. This disruption was incomplete, and stable at 300 MPa, independent of pressure history. At intermediate pressures, pressure history, (step-wise increase from ambient, or stepwise decrease from 300 MPa) had a strong effect on the scattering patterns. At high pressures, where scattering patterns were sufficiently structured, sizes of scattering entities could be deduced. The scattering entities at high pressure showed a bimodal size distribution. One size was outside the window of quantitative observation and may be similar to that of the native micelles or residual fat globules, the other smaller size, found under high pressure is in the 10–20 nm range and may correspond clusters of about 10 separate casein molecules. The pressure-induced disruption of casein micelles is partially reversed after return to ambient pressure, but small scattering entities, absent before pressure treatment, remain.

**Keywords** Casein micelles · Neutron scattering · High pressure · Milk

---

R. H. Tromp (✉) · T. Huppertz  
NIZO food research, Kernhemseweg 2,  
6718 ZB Ede, The Netherlands  
e-mail: hans.tromp@nizo.com

R. H. Tromp  
Van't Hoff laboratory for Physical and Colloid Chemistry, Debye  
Institute for Nanomaterials Science, University of Utrecht,  
Padualaan 8, 3584 CH Utrecht, The Netherlands

J. Kohlbrecher  
Laboratory for Neutron Scattering, CH-5232 Villigen PSI,  
Switzerland

## Introduction

Casein micelles contain 80 % of the protein in milk. Apart from being the main source of protein for the neonate they contain also essential amounts of calcium. Casein micelles are ingenious multifunctional non-covalent complexes of protein and nanoclusters of insoluble calcium phosphate. They offer a solution for the neonate's conflicting demands of high protein content, low viscosity for drinkability and sufficient bioavailable  $\text{Ca}^{2+}$ . The radius of casein micelles is between 50 and 200 nm, and they are stable in suspension in milk serum, giving skimmed milk its white appearance. Casein micelles are held together by a combination of hydrophobic interactions between protein molecules and ionic interactions between protein molecules and the calcium phosphate nanoclusters [1]. While casein micelles in general show a high stability to many physical treatments, the application of high pressures, >100 MPa, can have strong effects [2]. High pressure treatment of milk and related products has shown some commercially interesting applications, for instance in improving the rennet coagulation properties of milk [3–5], the strength of milk gels in cheesemaking [3, 4] and yoghurt-making, cheese yield [3, 5], and the texture and melting properties of ice cream [6]. As most of these changes in functional properties are related to pressure-induced changes in casein micelles [3–6], understanding of pressure-induced changes in casein micelles is required.

Observations on high pressure-treated skim milk show a lower turbidity, which is accompanied by a reduced average radius of the casein micelles and an increased amount of non-sedimentable caseins [2, 3]. To elucidate the underlying mechanisms responsible for the pressure-induced changes in casein micelles, in-situ studies have been performed where casein micelles suspensions were studied under pressure using light scattering. These studies highlight the reductions in intensity of scattered light and increases in the intensity of transmitted

light. The extent of these increases is larger at higher pressures and lower temperatures and is also affected by pH, mineral content and the concentration of casein micelles [7–10]. Calcium phosphate solubility increases with increasing pressure, leading to the solubilisation of considerable amounts of CCP [11, 12], which is expected to cause micellar disruption [7–10]. In contrast to whey proteins, caseins do not denature [13] and pressure-induced interactions between casein molecules are mostly enhanced at pressures >200 MPa [14, 15], suggesting that reduced protein interactions are unlikely to be the driving force behind pressure-induced disruption of casein micelles.

Small angle neutron scattering (SANS) offers considerable benefits for studying casein micelles at high pressure [16]. SANS is ideally suited, due to the low absorption of neutrons, for dealing with the thick container walls of a high pressure cell. Furthermore, when using D<sub>2</sub>O as a solvent, the contrast between non-deuterated casein micelles and the solvent allows easy observation of micelles and their disintegration. SANS was carried out while varying the pressure between ambient and 300 MPa. Three experiments were done:

1. Fast increase to 300 MPa and slow decrease to ambient, in equilibrated steps of 45–60 min.
2. Slow, step wise increase from ambient to 300 MPa in equilibrated steps of 45–60 min
3. Equilibration at 300 MPa, and fast release of the pressure to ambient, while monitoring the scattering in counting periods of 3 min.

In experiments 1 and 2, the pressure could be measured at which disintegration and reassembling takes place, and the products of the disintegration could be observed. Experiment 3 was carried out to follow the development in time of high pressure structure to (meta)stable structure at ambient pressure.

## Experimental

A fat-free and serum protein-free suspension of casein micelles was prepared by suspending the pellet obtained from ultracentrifugation (100,000 for 60 min at 20 °C) of milk from one individual cow in the 10 kDa permeate from the same milk. Using this approach, whey proteins and fat are omitted from the system as far as possible although the presence of small quantities cannot be excluded. The suspension, containing 7.2 % total solids and 1.8 % micellar casein, was freeze-dried. Prior to SANS measurements, the freeze-dried powder was suspended in D<sub>2</sub>O to obtain a micelle concentration of 1.8 % by weight, corresponding to a volume fraction of 0.024. As a consequence, the solvent was natural milk serum. The suspension was stirred during 1 h at room temperature and

stored at 4 °C. The casein free reference (for background subtraction) was a solution in D<sub>2</sub>O of 5.4 % dry freeze-dried 10 kDa permeate of milk. All percentages are on weight basis.

The neutron scattering experiments were carried out on the SANS-I beam line at the Swiss Spallation Neutron Source (SINQ), Paul Scherrer Institut, Villigen, Switzerland. The wavelength was 0.6 nm, the detector-sample distance 6 m and the Q-range probed was 0.03–0.6 nm<sup>-1</sup>. The scattering patterns were corrected for background scattering, absorption, empty cell and solvent scattering using the data processing software Grasp\_V6.25\_R2009b, provided by PSI. No absolute intensity scaling was applied. A pressure cell was used as described in Ref. [17]. This cell, equipped with sapphire windows and designed for pressures up to 500 MPa, was also suitable for light scattering, not employed for this work. However, by using this cell the turbidity of the casein suspension at various pressures was observed visually. All measurements were carried out at room temperature (approx. 23 °C).

## Results

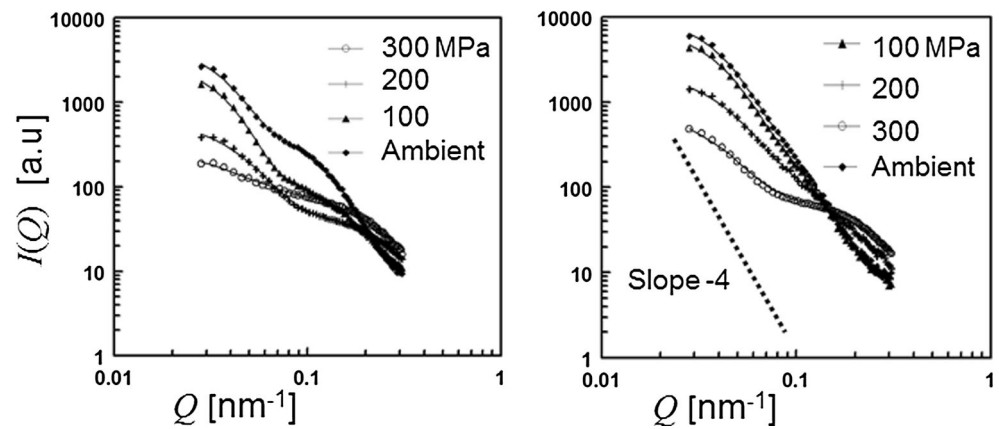
The general shape of the scattering intensities shown in Fig. 1 is a linear decay (in log-log representation) with a slope of approximately -4 (Porod behavior). This indicates the presence of large polydisperse scattering entities, with ‘large’ meaning that the radius of these entities is much larger than the reciprocal *Q* values probed. No size information of these entities can be obtained from the data presented here. Only deviations from the slope of -4 may contain size information. These deviations indicate the presence of scattering structure of a size within the reciprocal *Q* range probed, i.e. 10–100 nm.

At ambient pressure, before pressurizing, the only deviation from a slope of -4 is at *Q* values larger than 0.3 nm<sup>-1</sup>, and below 0.04 nm<sup>-1</sup>. The former is ascribed to the internal structure of the casein micelles, probably the structure in the spatial arrangement of calcium phosphate nanoclusters with a typical neighbour-neighbour distance of about 18 nm [1, 18]. The low-*Q* deviation from Porod behaviour reflects the fact that at this small *Q* value even the largest micelles, which dominate the scattering level, are not much larger than *Q*<sup>-1</sup>.

With increasing pressure, the smooth -4 slope is disturbed. An increase in scattering intensity is seen roughly at *Q* > 0.1 nm<sup>-1</sup>, and a decrease at *Q* < 0.1 nm<sup>-1</sup>. It can therefore be concluded that with increasing pressure, large scatterers disappear, and small scatterers are formed, or released from the disappearing larger structures. On return to ambient pressure after treatment at 300 MPa, the smooth -4 slope is not fully recovered, also not after hours of equilibration.

The increase and decrease of the scattering intensity at different *Q* values is more clearly seen in Fig. 2. It turns out that at low *Q* values, the effect of pressure is irreversible, and that it is reversible at high *Q* values (larger than app.

**Fig. 1** Scattering intensities at ambient and non-ambient pressures of 1.8 % casein micelles in milk serum with D<sub>2</sub>O as solvent. Equilibration at 300 MPa and stepwise descend to ambient pressure (left); Stepwise ascend from ambient pressure to 300 MPa (right). Time step approx. 1 h. The full lines are the fits corresponding to the size distribution shown in Fig. 3



0.2 nm<sup>-1</sup>). The total scattering is expressed by the scattering invariant:

$$I_{\text{tot}} = \int_{Q_{\text{min}}}^{Q_{\text{max}}} I(Q) Q^2 dQ \sim C \rho$$

where  $C$  is the scattering contrast and  $\rho$  is the number density of scattering entities.  $I_{\text{tot}}$  also shown in Fig. 2. Assuming that the contrast is independent of pressure, a decrease in  $I_{\text{tot}}$  can be considered a measure for the degree in which scattering entities dissolve and ‘disappear’ from the observation window set by the available  $Q$ -range between  $Q_{\text{min}}$  and  $Q_{\text{max}}$ . It turns out that  $I_{\text{tot}}$  is quite independent of the pressure, indicating that the total amount of scattering material observed in the present  $Q$  range is fairly constant, in spite of the changes in size distribution. However, a small but significant reduction in  $I_{\text{tot}}$  is observed between 100 and 200 MPa.

The deviation at non-ambient pressure from a slope of  $-4$  in Fig. 1 is a shoulder, shifting to higher  $Q$  values with increasing pressure. Considering the fact that the volume fraction of micelles is only about 2.4 %, this shoulder cannot be interpreted in terms of inter-micelle structure formation. Therefore, the shoulder suggests the formation of a population of smaller scattering entities, in shape well distinguishable from the large entities, which are only observable through the overall slope of  $-4$ . In order to further interpret this shoulder, the smoothest size distribution of spherical scatterers was sought, using Monte-Carlo routine, the calculated scattering pattern of which fitted the measured  $Q$ -dependent scattering. It was assumed that all scattering entities were spherical, with the same refractive index. The results for the cases of stepwise increasing and decreasing pressure are shown in Fig. 3, and the corresponding fits to the  $Q$ -space data are included in Fig. 1. The shoulder is transformed into a peak in the range 10–20 nm. At larger distance, an upturn is seen due the presence of scattering entities that are too large to be

quantified in the present data. The distributions are volume-weighted. A significant difference is observed for two cases of pressure variation.

The data shown in Figs. 1, 2 and 3 were collected after approximately 1 h of equilibration, when no further change between consecutive 3 min scattering runs could be observed.

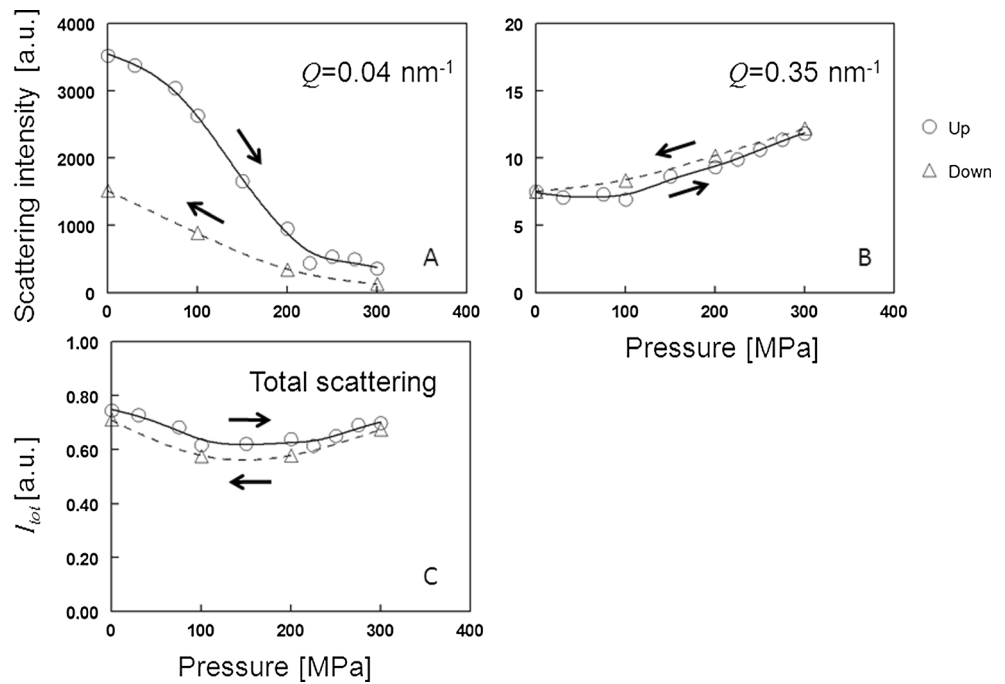
The change in scattering pattern, amounting to a lowering of the scattering intensity and a shift to higher  $Q$  values, takes place simultaneously with optical transparency of the micelle suspension. As shown in Fig. 4, this transparency is maintained after decompression from 300 MPa.

Figure 5 shows the results, both in  $Q$  and real space for the development of the structure after a sudden (less than 1 min) release of the pressure of 300 MPa. Qualitatively, the same picture as for slow release is seen, with a shoulder near  $Q=0.1$  nm<sup>-1</sup> and a fairly constant  $I_{\text{tot}}$ .

## Discussion

The picture which appears is that of a decomposition of large scattering entities, which starts already at the lowest non-ambient pressures which were tested (Fig. 2). At higher pressures (above 100 MPa) a shoulder appears, which corresponds to an emerging scattering structure smaller than about 30 nm (a larger emerging structure, which may already be there at lower non-ambient pressure cannot be resolved from the ‘native’ large scattering entities). This structure decreases in size to about 10 nm with the pressure increasing to 300 MPa. Slow (in equilibrated steps of 1 h) and fast (in a few minutes) exposure to increase from ambient to 300 MPa leads to approximately the same emerging structure of 10 nm (Fig. 3). Also, the large structures, probed at  $Q=0.04$  nm<sup>-1</sup> are the same at 300 MPa reached either slowly or fast. However, the structures at intermediate pressures are different for ascending and descending step-wise pressure histories (Figs. 2 and 3). The structures formed after slow downward pressure steps are more pronounced than those formed after upward steps.

**Fig. 2** The scattering intensity at low (a) and high (b)  $Q$  values with increasing and decreasing pressure, and total scattering (c). The curves are aides to the eye. Downward: equilibration at 300 MPa and stepwise descend to ambient pressure; Upward: stepwise ascend from ambient pressure to 300 MPa. Time step approx. 1 h. It should be noted that the upward and downward pressure series were recorded with different samples.



Although the increasing pressure causes a decrease in low  $Q$  scattering intensity and increase in high  $Q$  scattering, an overall negative slope in the scattering pattern remains, indicating that the large entities only partially decompose. The visual transparency after high pressure, indicating the disappearance of large scattering particles (larger than 500 nm) shown in Fig. 4 may therefore not be directly related to observations from neutron scattering. The change in light scattering may rather be more due to dissolution of casein aggregates, still remaining after dispersion of the powder. Of course, the dissolution of aggregates at high pressure will be dependent on instability of casein in this condition. A small number of residual fat globules, often found in skimmed milk, may also contribute to the turbidity at high pressure.

The observations from neutron scattering with increasing pressure suggest the partial disruption of native casein micelles into smaller structures, stable at 300 MPa. This is seen during slow, stepwise decrease, but also in time after a quench toward ambient pressure (Fig. 5). After the quench, the small,

pressure-induced structure grows in size and becomes more pronounced. The final structure at ambient pressure after about two hours is characterized by the presence of small structure, which did not exist before the exposure to high pressure.

The development of the scattering pattern with the pressure, both during slow (Fig. 1) and fast change (Fig. 5) shows a constant region, perhaps even an isosbestic point at  $0.19 \text{ nm}^{-1}$ . An isosbestic point is a concept from spectroscopy (<http://goldbook.iupac.org/I03310.html>) and would indicate here, either in real or in reciprocal space, the presence of two populations of scattering objects differing in size and developing in time their number ratio, but not their sizes. In this case the two types of scattering objects appear to be present: one larger than roughly 30 nm and one smaller than roughly 30 nm. The picture of two types of scattering entities, one stable at ambient pressure, and the other stable at 300 MPa, may explain the observed total scattering (in the  $Q$ -range probed), shown in Figs. 2c and Fig. 5b. At

**Fig. 3** Size distribution fitting the shoulder in the data in Fig. 1

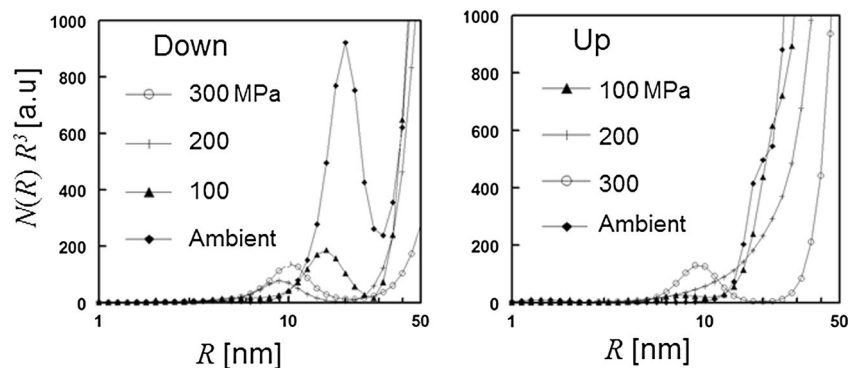
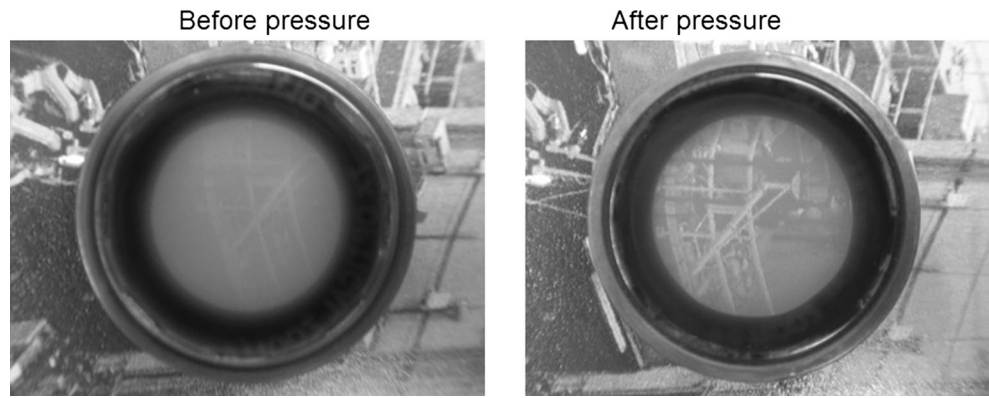


**Fig. 4** High pressure sample container at ambient pressure filled with 1.8 % a case in micelle suspension before and after pressurizing at 300 MPa. The outer diameter of the cell is 3 cm

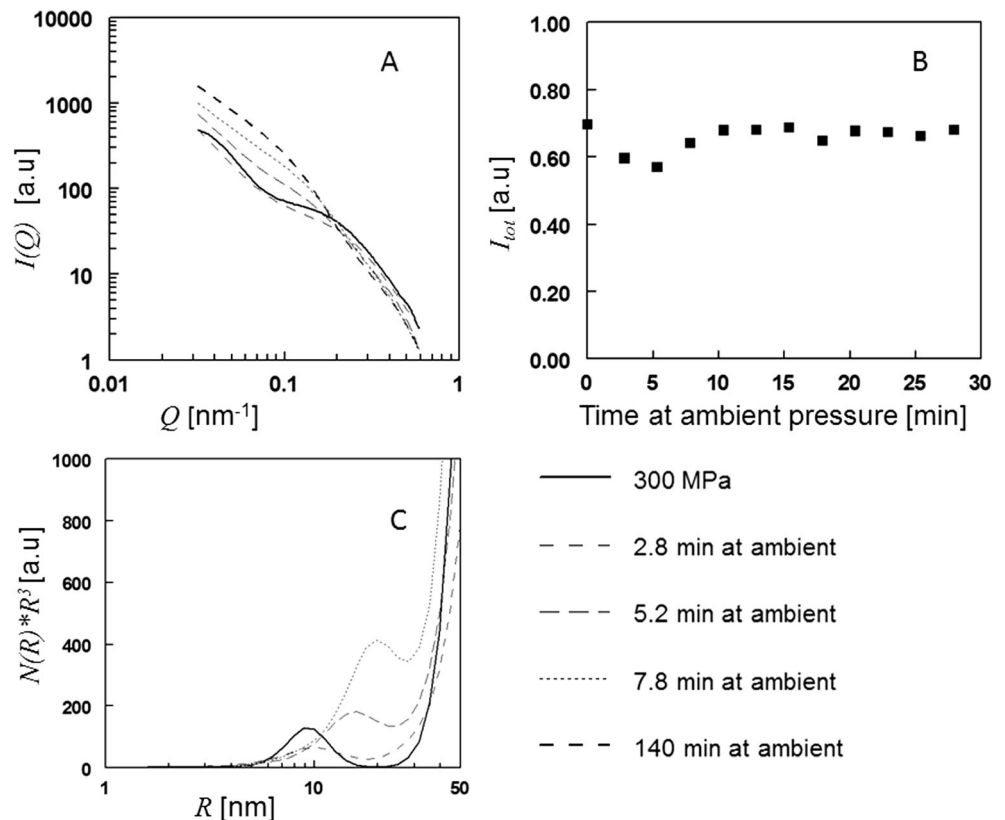


intermediate pressures (100–200 MPa), as well as after a sudden decrease from 300 MPa, the total scattering is lower than at ambient or 300 MPa. This could be explained by dissolution of one type of scatterers, whereas the other type has not yet formed (either due to insufficient pressure or insufficient time).

A bimodal distribution is in accordance with Ref. [16], where the appearance of small scattering entities was interpreted as the desintegration of casein micelles producing submicelles, believed to be the building blocks of the intact micelles. This interpretation differs slightly from that of the present data, which appears to show an increase of number of the small scattering entities, which therefore are not referred to as ‘submicelles’. The dissolution of calcium

phosphate at high pressure may in our view play a dominant role. A two size distribution was also reported in Ref. [19], although there the existence of the population was derived from static light scattering techniques, which will not detect structures of 30 nm or smaller. From dynamic light scattering at pressures up to 400, decomposition into scattering entities of 30 nm was concluded [20], in accordance with the neutron results. Full disruption was observed at 300 MPa, whereas the results presented here show a significant scattering due to scatterers larger than 30 nm remaining. This discrepancy might be explained by the fact that in the buffer used as a solvent in Refs [19, 20]. Ca-phosphate was not present at saturation. Furthermore, casein concentration and type of buffer were not the same as in the experiments presented in

**Fig. 5** Structure development after release of a pressure of 300 MPa. Scattering intensity patterns (smoothed) during the first 8 min at ambient pressure (a), total scattering during the first half hour at ambient pressure (b) and the size distribution of the scattering entities responsible for the shoulder in the scattering pattern (c)



this paper. Therefore, a detailed, quantitative comparison is not feasible.

## Conclusions

The disruption due to high pressure (up to 300 MPa) of casein micelles in milk serum was followed by small angle neutron scattering. This disruption is incomplete, and leads to a bimodal size distribution. One size is similar to that of the original micelles, the other, only stable at high pressure, is in the range of 20 to 40 nm in diameter. The disruption by high pressures is only partially reversible on return to ambient pressure. A sudden release of a pressure of 300 MPa triggered the growth of small scattering entities, their size apparently being destabilized by the drop in pressure. The characteristic time scale of both disruption at 300 MPa and reassembling at ambient pressure of the micelles was found to be in the order of 10 min.

## References

1. C.G. de Kruif, T. Huppertz, V.S. Urban, A.V. Petukhov, *Adv. Coll. Interf. Sci.* **171**, 36–52 (2012)
2. T. Huppertz, P.F. Fox, K.G. de Kruif, A.L. Kelly, *Biochim. Biophys. Acta* **1764**, 593–598 (2006)
3. R. López-Fandiño, *Int. Dairy J.* **16**, 1119–1131 (2006)
4. M.R. Zobrist, T. Huppertz, T. Uniacke, P.F. Fox, A.L. Kelly, *Int. Dairy J.* **15**, 655–662 (2005)
5. T. Huppertz, M.A. Smiddy, V.K. Upadhyay, A.L. Kelly, *Int. J. Dairy Technol.* **59**, 58–66 (2006)
6. T. Huppertz, M.A. Smiddy, H.D. Goff, A.L. Kelly, *Int. Dairy J.* **21**, 718–726 (2011)
7. T. Huppertz, C.G.J. De Kruif, *Agr. Food Chem.* **54**, 5903–5909 (2006)
8. T. Huppertz, A.L. Kelly, C.G.J. de Kruif, *Dairy Res.* **73**, 294–298 (2006)
9. V. Orlien, J.C. Knudsen, M. Colon, L.H. Skibsted, *Food Chem.* **98**, 513–521 (2006)
10. V. Orlien, L. Boserup, K.J. Olsen, *Dairy Res.* **93**, 12–18 (2010)
11. C.D. Hubbard, D. Caswell, H.D. Lüdemann, M.J. Arnold, *Sci. Food Agric.* **82**, 1107–1114 (2002)
12. T. Huppertz, C.G. de Kruif, *Colloid Surf. A.* **295**, 264–268 (2007)
13. M. Paulsson, P.J. Dejmek, *Dairy Sci.* **73**, 590–600 (1990)
14. T.J. Payens, K. Heremans, *Biopolymers* **8**, 335–345 (1969)
15. D.G. Schmidt, T.A.J.J. Payens, *Colloid Interface Sci.* **39**, 655–662 (1972)
16. A.J. Jackson, D.J. McGillivray, *Chem. Comm.* **47**, 487–489 (2011)
17. J. Kohlbrecher, A. Bollhalder, R. Vavrin, G. Meier, *Rev. Sci. Instrum.* **78**, 125101 (2007)
18. C. Holt, C.G. De Kruif, R. Tuinier, P.A. Timmins, *Colloid Surf. A.* **213**, 275–284 (2003)
19. R. Gebhardt, N. Takeda, U. Kulozik, W.J. Doster, *Phys. Chem. B* **115**, 2349–2359 (2011)
20. R. Gebhardt, W. Doster, J. Friedrich, U. Kulozik, *Eur. Biophys. J.* **35**, 503–509 (2006)